JOURNAL OF GEOPHYSICAL RESEARCH, VOL. 115, A06319, doi:10.1029/2009JA014694, 2010

A comparison of EISCAT and SuperDARN *F*-region measurements with consideration of the refractive index in the scattering volume

R. G. Gillies,[1] G. C. Hussey,[1] G. J. Sofko,[1] D. M. Wright,[2] and J. A. Davies[3]

Received 28 July 2009; revised 11 December 2009; accepted 12 February 2010; published 30 June 2010.

[1] Gillies et al. (2009) proposed the use of interferometric measurements of the angle of arrival as a proxy for the scattering region refractive index n_s needed to estimate the line-of-sight Doppler velocity of the ionospheric plasma from HF [Super Dual Auroral Radar Network (SuperDARN)] radar observations. This study continues this work by comparing measurements of line-of-sight velocities by SuperDARN with tristatic velocity measurements by the EISCAT incoherent scatter radar from 1995 to 1999. From a statistical viewpoint, velocities measured by SuperDARN were lower than velocities measured by EISCAT. This can, at least partially, be explained by the neglect in the SuperDARN analysis of the lower-than-unity refractive index of the scattering structures. The elevation angle measured by SuperDARN was used as a proxy estimate of n_s and this improved the comparison, but the velocities measured by SuperDARN were still lower. Other estimates of n_s using electron densities N_e based on both EISCAT measurements and International Reference Ionosphere model values did not increase the SuperDARN velocities enough to attain the EISCAT values. It is proposed that dense structures that were of comparable size to the SuperDARN scattering volume partially help resolve the low-velocity issue. These dense, localized structures would provide the N_e gradients required for generation of the coherent irregularities from which the SuperDARN radar waves scatter, whereas EISCAT incoherent radar measurements provide only the background N_e and not the density of the small-scale structures. The low-velocity SuperDARN results suggest that small-scale dense structures with refractive indices well below unity must exist within the SuperDARN scattering volume and may contribute greatly to the scattering process.

Citation: Gillies, R. G., G. C. Hussey, G. J. Sofko, D. M. Wright, and J. A. Davies (2010), A comparison of EISCAT and SuperDARN *F*-region measurements with consideration of the refractive index in the scattering volume, *J. Geophys. Res.*, *115*, A06319, doi:10.1029/2009JA014694.

1. Introduction

[2] In the paper by *Gillies et al.* [2009] the concept of using angle-of-arrival measurements as a proxy for refractive index n_s in the local scattering region of a high-frequency (HF) radar was introduced. As outlined below, this allows for a better line-of-sight Doppler velocity estimate to be made by the Super Dual Auroral Radar Network (SuperDARN) [*Greenwald et al.*, 1995] HF radar system. Due to the large field-of-view required for global convection measurements by radar systems such as SuperDARN, the small-scale resolution needed to determine the refractive index n_s at the scattering location is not possible. The detailed electron density measurements needed to determine n_s are not readily available. The result is that estimates of refractive index have been unavailable for use in the Doppler velocity analysis, so a default value of 1.0 is usually used.

[3] Line-of-sight velocities v_s measured by SuperDARN are calculated using the following equation:

$$v_s = \frac{\Delta\omega_D v_p}{2\omega} = \frac{\Delta\omega_D}{2\omega}\frac{c}{n_s}, \tag{1}$$

where $\Delta\omega_D$ is the Doppler shift, v_p is the phase speed of the radar wave in the scattering region, ω is the radar wave frequency [*Baker et al.*, 1995], c is the speed of light in a vacuum, and n_s is the refractive index in the scattering region [*Ginzburg*, 1964]. Recent work by *Gillies et al.* [2009] has demonstrated that n_s will be typically around 0.8 or 0.9, so the default value of 1.0 leads to systematic underestimation of the Doppler velocity.

[4] The determination of the local refractive index for a given SuperDARN echo allows an improved line-of-sight

[1] Institute for Space and Atmospheric Studies, University of Saskatchewan, Saskatoon, Saskatchewan, Canada.
[2] Department of Physics and Astronomy, University of Leicester, Leicester, UK.
[3] Space Science and Technology Department, Rutherford Appleton Laboratory, Didcot, UK.

0148-0227/10/2009JA014694

velocity estimate to be made by application of equation (1). The most direct method to estimate n_s is to use local electron density N_e measurements or estimates and directly calculate the refractive index using the Appleton-Hartree equation [*Budden*, 1961]. This can be done if there is an instrument such as an ionosonde or incoherent scatter radar to measure N_e. Unfortunately, the field of view of a given SuperDARN radar is quite large (~4 million km^2) and it is impossible to have instruments that measure N_e continuously throughout this region. Electron densities can also be estimated using the International Reference Ionosphere (IRI) model [*Bilitza*, 2001], which can provide a mean estimate of N_e at any location. However, these estimates are based on empirical models and do not account for the small-scale structures that are responsible for the majority of SuperDARN scattering.

[5] *Gillies et al.* [2009] proposed a method to determine n_s using elevation angle data from SuperDARN as a proxy for the refractive index in the scattering region. The equation relating n_s to the angle of arrival or elevation angle was:

$$n_s = \frac{R_E}{(R_E + h_s)} \frac{\cos \phi_o}{\sin \psi}, \tag{2}$$

where R_E is the radius of the Earth, h_s is the altitude of the scattering point, ψ is the magnetic dip angle at the scattering point, and ϕ_o is the elevation angle measured by SuperDARN. The benefit of this method is that it does not rely on the existence or reliability of other instruments for an n_s estimate.

[6] Previous studies have consistently demonstrated that, on a statistical basis, SuperDARN measured line-of-sight velocities were lower than velocities derived from other instruments. For example, F-region drift velocities as measured by DMSP satellites and SuperDARN were compared by *Drayton et al.* [2005] and *Drayton* [2006]. The *Drayton et al.* [2005] study compared velocities over the period of 1999–2003 and found that the best fit line to the data had a slope of 0.72 (SuperDARN velocities were, on average, lower). A magnetic dipole field-mapping correction of the electric field was then made to this data set in *Drayton* [2006] to account for the fact that DMSP measured velocities at ~840 km and SuperDARN measured velocities at ~250 km. This correction effectively decreased the higher altitude DMSP calculated velocity values and the slope of the best fit line increased to 0.84.

[7] Work by *Gillies et al.* [2009] continued the SuperDARN-DMSP comparison by examining comparison points in which SuperDARN data had an accompanying elevation angle. This reduced the number of comparison points and the best fit slope of this subset was 0.74. It was suggested that the reason for the lower slope value compared to *Drayton* [2006] was that the subset of points with elevation angle information was predominantly situated in the auroral zone where there were typically higher electron densities and more complex structures, while the full data set was significantly weighted with more observations in the polar cap region, where lower electron densities and less complex structures prevail. Nonetheless, when equation (2) was applied to obtain an estimate of n_s, the slope of the best fit line increased to 0.83, about a 12% improvement, indicating that the SuperDARN velocities, although better estimated, were still systematically lower than DMSP velocities.

[8] Studies of comparisons between velocities measured by SuperDARN and velocities measured by incoherent scatter radars have also been performed. Velocities measured by SuperDARN and by the Sondrestrom incoherent scatter radar were compared by *Xu et al.* [2001], resulting in a best fit slope of only 0.42. *Eglitis et al.* [1998] compared tristatic ion drift measurements from the European Incoherent Scatter (EISCAT) UHF radar [*Rishbeth and van Eyken*, 1993] to line-of-sight measurements from the Hankasalmi SuperDARN radar. This study utilized an ionospheric heater [*Robinson*, 1989; *Rietveld et al.*, 1993; *Stubbe*, 1996, and references therein] to generate artificial irregularities that the Hankasalmi SuperDARN detected. It was found that there was very good agreement between velocity values when the heater was on (the best fit line to the data had a slope of 1.02). Using scatter from irregularities that were natural, rather than artificially generated by a heater, a comparison of EISCAT and SuperDARN velocities was performed by *Davies et al.* [1999] over the period of 1995–1997. This study led to a best fit line with a slope of 0.72. The present study expands the above comparison made by *Davies et al.* [1999] to include data from 1998 and 1999, thereby improving the overall statistical database.

2. Experiment Overview

[9] The first of the two instruments used in the present study was the SuperDARN radar located at Hankasalmi, Finland. SuperDARN is a collection of radars that monitor high latitude ionospheric convection in both the Northern and Southern Hemispheres using coherently scattered HF signals in the 8–20 MHz range [*Greenwald et al.*, 1995]. A SuperDARN radar, in its common mode, consists of a main array of 16 antennas that are phased to sample 16 successive beam directions in steps of 3.24°, covering a total of ~52° in azimuth. The radars are routinely configured such that each beam samples 75 different range gates, each with 45 km resolution. In normal operation, each beam is scanned in sequence for 3 s or 7 s, so a full scan of all 16 beams is performed every 1 or 2 min, respectively. An interferometer array of four antennas is also located 100 m behind or in front of the main array at each SuperDARN radar site. The cross-correlation between the signal received by the interferometry array and the main array is used to determine the elevation angle of the returned echo [*Milan et al.*, 1997; *André et al.*, 1998]. The Hankasalmi SuperDARN radar is located at the geographic location 62.3°N, 26.6°E (geomagnetic coordinates: 59.8°N, 105.5°E). The central pointing direction of this radar is 12.0° west of geographic north.

[10] The second instrument used in this study is the EISCAT UHF incoherent scatter radar facility [*Rishbeth and van Eyken*, 1993]. The EISCAT system operates at 931 MHz and consists of three parabolic dish antennas located in Tromsø (Norway), Kiruna (Sweden), and Sodankyla (Finland). The antenna in Tromsø has both transmit and receive capabilities, while the other two antennas operate as passive receivers. The data considered in this study resulted from times when EISCAT was running the common program modes CP-1 and CP-2.

[11] The CP-1 mode consisted of the transmitter at Tromsø oriented to point along a fixed path antiparallel to the local

magnetic field lines (~77° elevation). The antenna beam had a half-power width of 0.6° which corresponds to a width resolution of roughly 7 km at a measurement altitude of 280 km. The Tromsø radar sampled with an altitude resolution of 22 km along the beam from 150 km to 600 km. The two remote sites and the Tromsø antenna received signal from a common intersection volume at an altitude of ~280 km centered at 69.1°N, 19.1°E, which corresponded to beam 5 and range gate 16 of the Hankasalmi SuperDARN radar. The signal received at each EISCAT site was integrated over 5 s, and then these 5 s intervals were post-integrated over 2 min. The result of each integration was a velocity vector for each of the three antennas. The Tromsø velocity vector was along the antenna beam, while the remote receiver velocity vectors were along the bisector between the Tromsø beam and the remote receiver beams. These three velocity vectors allow determination of the full velocity vector within the intersection volume. The component of the full EISCAT velocity vector was then resolved along the Hankasalmi SuperDARN radar line-of-sight direction and the velocity values from the two instruments were directly compared.

[12] The CP-2 mode was nearly identical to the CP-1 mode except that four different intersection volumes were scanned in a period of 6 min so each position had a post-integration time of 90 s. These positions consisted of the Tromsø beam transmitting along the field lines (identical to the position of the CP-1 mode), vertically, and in two different southeastward directions. The geographic locations of each of these positions were as follows: (1) 68.7°N, 21.8°E (Hankasalmi beam 7, range gate 14); (2) 68.4°N, 20.0°E (Hankasalmi beam 5, range gate 14); (3) 69.1°N, 19.1°E (Hankasalmi beam 5, range gate 16); and (4) 69.6°N, 19.2°E (Hankasalmi beam 5, range gate 17). Note that the four CP-2 positions were relatively close to each other and only extended from Hankasalmi range gates 14 to 17.

3. Statistical Velocity Comparisons

3.1. Initial Comparison

[13] All the CP-1 and CP-2 velocity measurements from 1995 to 1999 during periods with simultaneous Hankasalmi SuperDARN velocity data have been compared. Both in order to filter out SuperDARN *E*-region velocities and, more importantly, to improve the SuperDARN measurements by taking the index of refraction into account, only SuperDARN echoes with available elevation angle information were used. SuperDARN velocities that were less than 50 m/s or that had a signal-to-noise ratio less than 3 dB were discarded. Typically, the SuperDARN radar performed 2 min scans so the 2 min EISCAT integration time of the CP-1 mode was coincident with the SuperDARN scan time. On some occasions, SuperDARN was operating in a special mode with shorter scans or in the 1 min scan mode. In these cases, any SuperDARN values that were within the EISCAT scan time were averaged. For the CP-2 mode, EISCAT integrated at each position for 90 s and the data observations were compared when any part of the SuperDARN scan overlapped with any part of the EISCAT integration and, as such, temporal alignment was not often ideal.

[14] From 1995 to 1999 there were 11 CP-1 experiments that varied in length between 2 and 5 days and 10 such experiments in the CP-2 mode. In total, over 1300 velocity comparisons were performed using the criteria discussed above, and these were split roughly equally between CP-1 and CP-2 types (658 and 668, respectively). This velocity comparison between EISCAT and SuperDARN is presented as Figure 1. EISCAT velocities are plotted along the horizontal axis and SuperDARN velocities are plotted along the vertical axis. The best fit line to the data is also plotted as the solid line. The immediate issue with this comparison is the low correlation coefficient $r = 0.39$. This is due to the large collection of points along the vertical axis, which correspond to very low EISCAT velocities and a large range of SuperDARN velocities.

3.2. Removal of *E*-Region and Noisy Data

[15] In order to check the reliability of the SuperDARN data in a given range cell, the surrounding eight cells in a 3 × 3 grid were examined. Points were discarded if more than four of these cells did not record data or the standard deviation of velocity in all considered cells (up to a maximum of nine cells) was greater than 50% of the velocity average of the cells. Note that the single SuperDARN velocity value of the cell under consideration (not the average velocity of the nine cells) was the value used for comparison with the EISCAT velocity value. The results of this filtering are presented in Figure 2 and it is apparent that most of the anomalous data has been removed. Some 40% of the original points have been discarded. The correlation coefficient has risen to 0.91 and the slope of the best fit line has risen from 0.66 to 0.78.

[16] The next step in the comparison was to filter out any SuperDARN echoes that may be *E*-region scatter. In contrast to the *F* region, convection in the *E* region is limited to the ion-acoustic velocity (400–600 m/s) [*Haldoupis and Schlegel*, 1990] and thus *E*-region SuperDARN velocities would not agree with *F*-region EISCAT velocities. To distinguish *E*-region velocities from *F*-region velocities, the distribution of elevation angles was examined as presented in Figure 3. The majority of the elevation angles that were observed in this study clustered around 25° with a much smaller cluster between 10° and 15°. The latter cluster is expected to be due to *E*-region backscatter. The SuperDARN echoes examined in this study all came from essentially the same range (from gates 14 to 17, inclusive). At this range, elevation angles of ~25° were appropriate for half-hop *F*-region scatter and elevation angles below ~15° were appropriate for *E*-region scatter. Therefore, echoes with elevation angles below 15° were considered to be from *E*-region altitudes and were discarded. This removed an additional 64 comparison points; however, the slope of the best fit line and the correlation coefficient did not change in the EISCAT-SuperDARN comparison (figure not shown).

[17] A further analysis of possible *E*-region contamination in the SuperDARN data set was performed by examining various SuperDARN low-velocity cutoff values. It was found that discarding SuperDARN velocities that were below various arbitrary cutoff values did not appreciably change the slope of the best fit line. The slope of the best fit line was examined for several low velocity cutoffs from 50 m/s to 600 m/s in 25 m/s increments and it was found that the best result was obtained when velocities which were less than 125 m/s were removed. Using this cutoff,

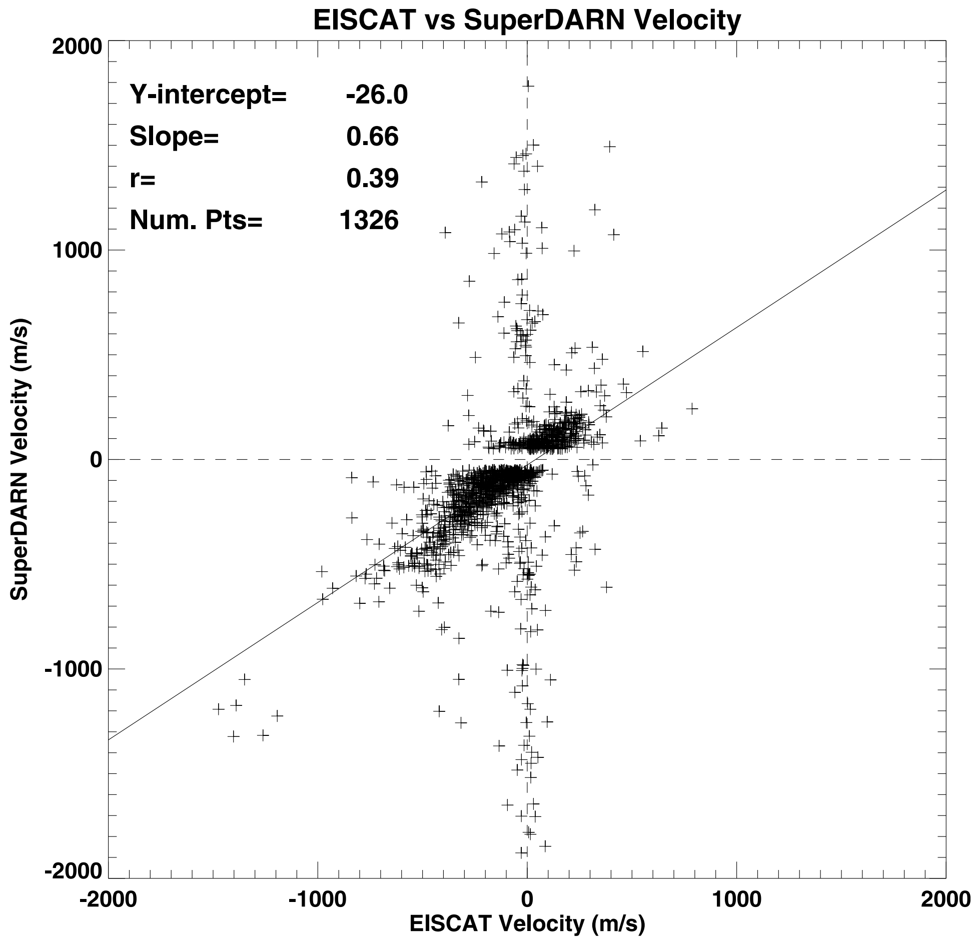

Figure 1. SuperDARN and EISCAT velocity comparison for EISCAT CP-1 and CP-2 modes from 1995 to 1999.

391 points were removed and the best fit slope increased from 0.78 to 0.81. However, since there is no basis for removing points with velocities below this arbitrary threshold (and the removal had little effect on the best fit slope), it was determined that the most accurate representation of F-region scatter was obtained using the elevation angle cutoff criteria which was discussed above.

3.3. Accounting for n_s in the SuperDARN Scattering Volume

[18] The slope of the best fit line when comparing the SuperDARN velocities to EISCAT velocities as presented in Figure 2 is 0.78 from 832 points (note that there were 768 points after the probable *E*-region echoes were removed). SuperDARN, on average, underestimated the ionospheric scatterer velocities; however, the measured velocities still need to be adjusted to account for the refractive index in the scattering region, n_s. Three different methods have been employed to determine an estimate of n_s for each comparison point.

[19] The first method is based on the electron density N_e values that the EISCAT Tromsø radar measured. In order to estimate n_s for SuperDARN, the maximum N_e measured along the Tromsø EISCAT beam was selected to represent the electron density in the local scattering volume. The Appleton-Hartree equation [*Budden*, 1961] was used to determine n_s from this N_e value. With this estimate for n_s, equation (1) was applied to determine SuperDARN velocities. The slope of the best fit line increased from 0.78 to 0.84, an increase of ~8%. It should be noted that in order for this method to deliver accurate results, a significant assumption has been made: the SuperDARN scatter came from the same location at which EISCAT measured the peak N_e. If the SuperDARN scatter location was offset in altitude from the peak electron density and/or the distribution of SuperDARN scatter within the range cell predominantly occurred in a different location than where EISCAT measured within the range cell, the estimate for n_s from this method will not accurately reflect the electron density at the scattering location. This altitude ambiguity and difference in the instrument scattering volumes will be discussed in more detail in section 4.

[20] The second method is also based on using electron density values to obtain an estimate for n_s. For this method, the IRI model was used to determine the peak N_e estimate at the time and location of the velocity measurement. Applying equation (1) to determine the SuperDARN velocity values with this approximation for n_s resulted in the slope of the best fit line increasing from 0.78 to 0.87, an increase of ~12%. Again, in the application of this method, the assumption was made that SuperDARN scatter occurred at the

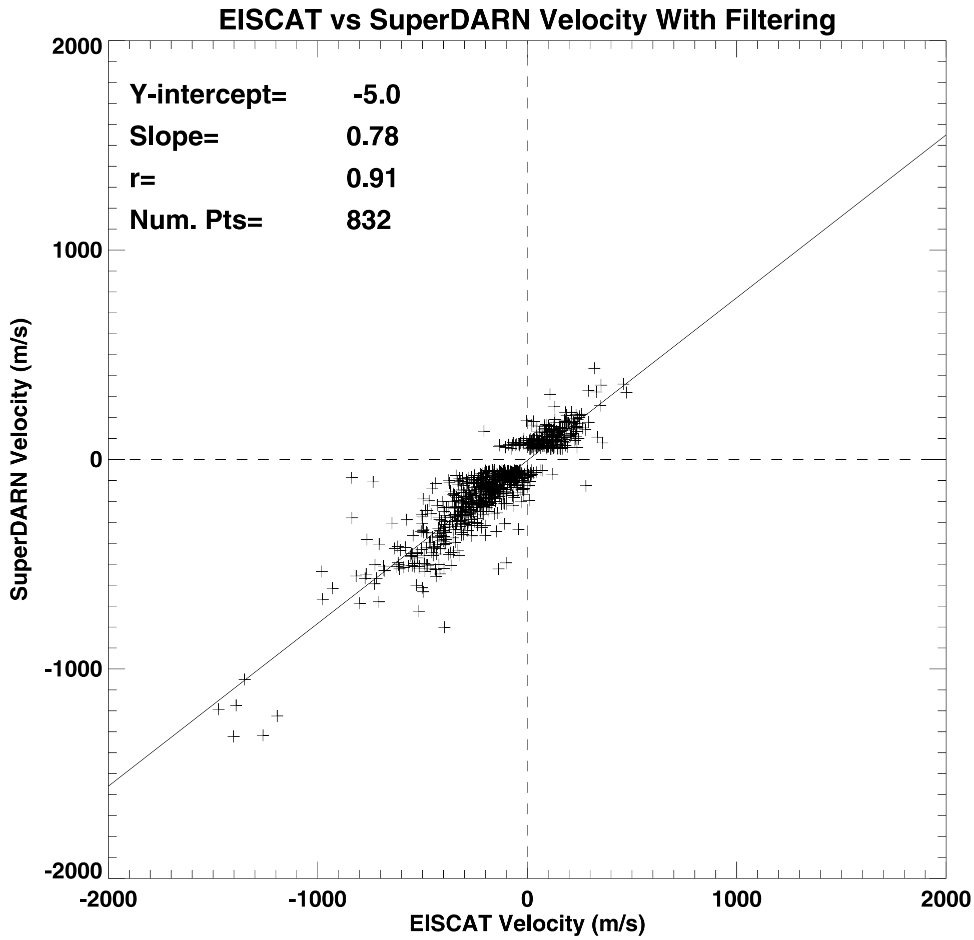

Figure 2. SuperDARN and EISCAT velocity comparison for EISCAT CP-1 and CP-2 modes from 1995 to 1999. SuperDARN points that showed either high standard deviation or little data in the surrounding cells were discarded.

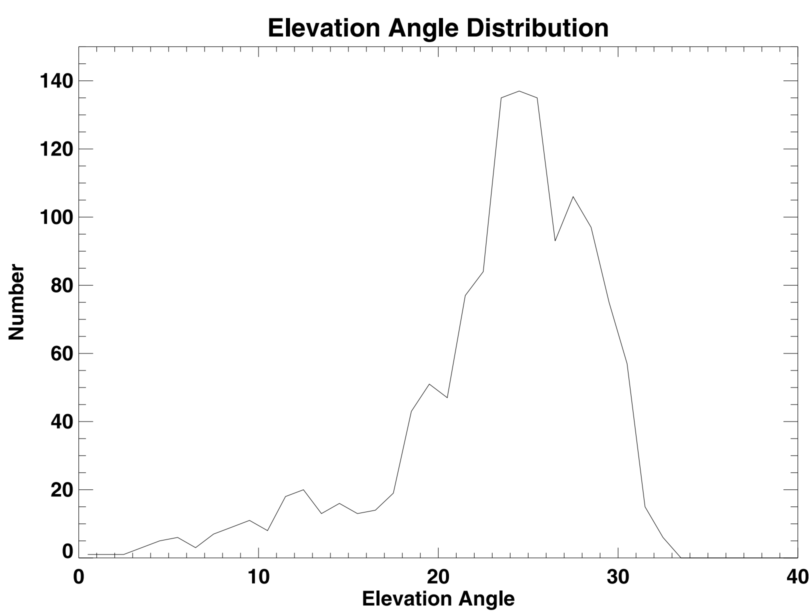

Figure 3. The number of data points with a given elevation angle.

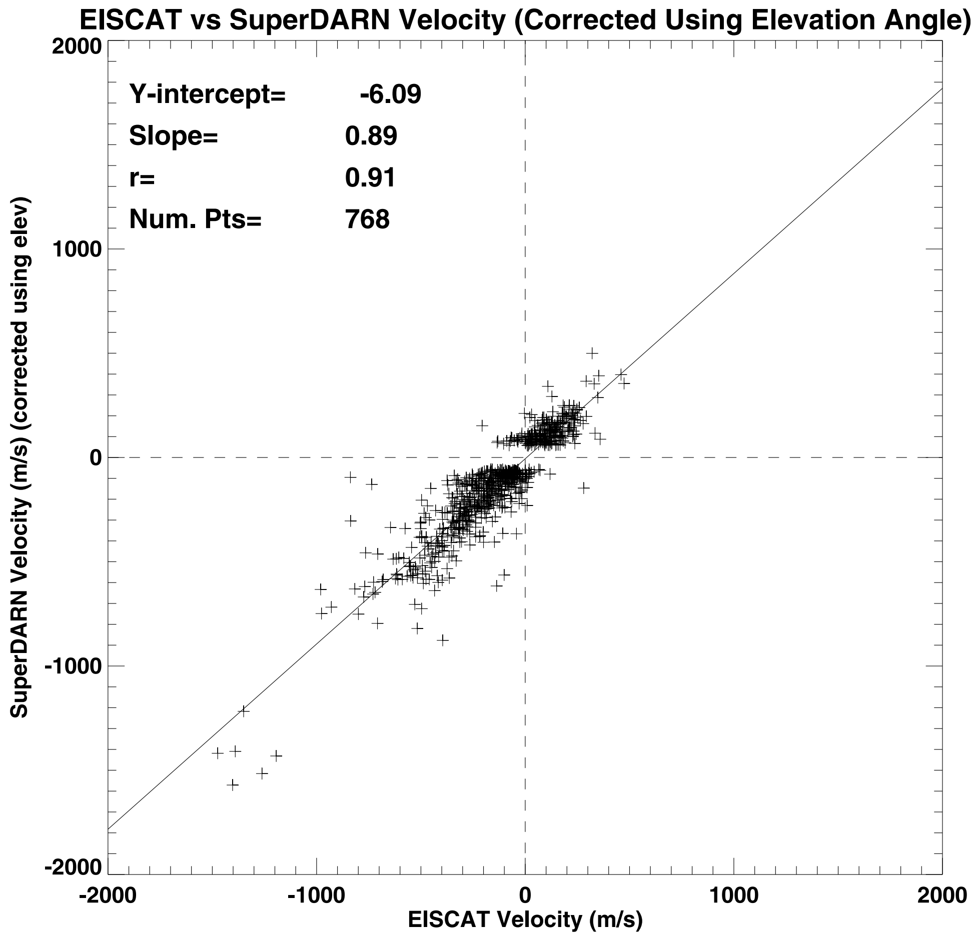

Figure 4. SuperDARN and EISCAT velocity comparison for EISCAT CP-1 and CP-2 modes from 1995 to 1999. SuperDARN points that showed either high standard deviation or little data in the surrounding cells were discarded. Also discarded were SuperDARN velocities that had elevation angles below 15° to remove *E*-region scatter. Finally, n_s was estimated and used to improve the SuperDARN velocities using equations (1) and (2).

F-region peak altitude. Further, the IRI uses empirical models and gives only a large-scale estimate of N_e so that any small-scale structures, which may be very important in the generation of field-aligned irregularities, will not be taken into account.

[21] The final method to determine an estimate for n_s exploits equation (2) and the elevation angle ϕ_o that SuperDARN was capable of measuring for each echo. Again, the estimate for n_s was used with equation (1) to improve each SuperDARN velocity measurement. The comparison between EISCAT and SuperDARN velocity values using the elevation angle as a proxy for n_s is presented as Figure 4. The result was an increase of the best fit slope from 0.78 to 0.89, an improvement of ~14%. The important assumption made with this approximation for n_s was that there were no horizontal gradients in N_e along the radar wave path. This was most likely not the case; nonetheless, a reasonable estimate of n_s is possible with this method (it is the best of the three presented here) and this method had the added benefit that the elevation angle was directly linked to the scattering location of SuperDARN and not of any other instrument whose target region may be displaced spatially and temporally from that of SuperDARN.

3.4. Comparison of n_s Values From Different Methods

[22] It is useful to compare directly the n_s values obtained from each different method. These methods measure the same parameter in the ionosphere, so in principle, they should provide the same average refractive index value and there should be high correlation between individual data points measured from each method. The mean refractive index predicted using the elevation angle proxy was 0.88 with a standard deviation of 0.02. Using EISCAT measurements of electron density provided a mean refractive index value of 0.92 with a standard deviation of 0.03. Finally, IRI estimates of electron density provided a mean refractive index value of 0.91 with a standard deviation of 0.05. These numbers indicate that, on average, use of any of the three presented methods to predict refractive index in the SuperDARN scattering region will provide results similar to the other two methods. A point-by-point comparison revealed that the correlation between the different measures

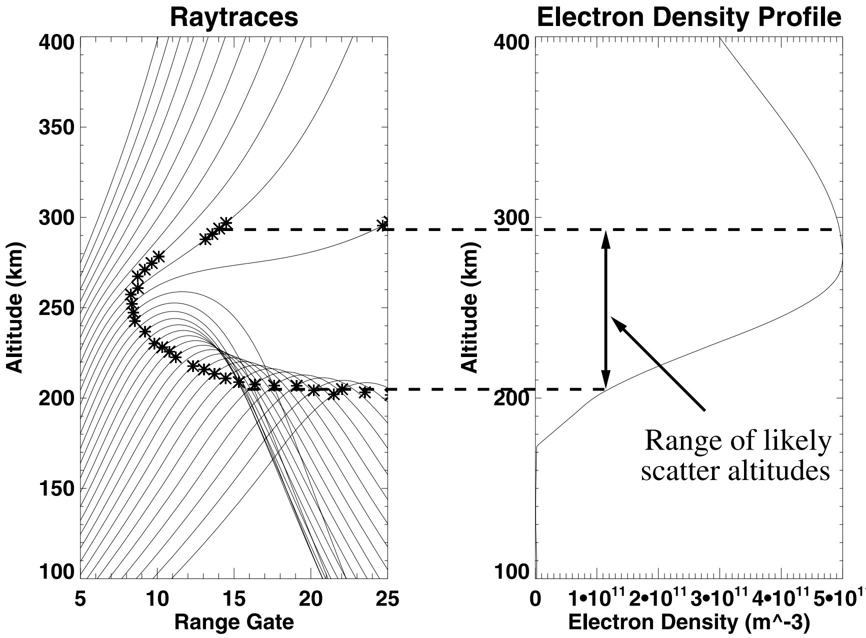

Figure 5. On the left are the raypaths from SuperDARN through the profile displayed on the right. The operating frequency was 12.5 MHz.

of n_s was low (e.g., estimates of n_s as derived from EISCAT N_e measurements and the elevation angle proxy estimate, when compared on a point-to-point basis, resulted in a correlation coefficient of 0.21). Comparisons between IRI and elevation angle estimates of n_s and between IRI and EISCAT estimates of n_s were lower. Possible explanations for this lack of correlation are discussed in the following section.

4. Discussion

4.1. Comparison Results

[23] Three different methods have been applied to account for refractive index in the SuperDARN velocity determinations. These methods increased the best fit slope between SuperDARN and EISCAT velocity measurements between 8% and 14%, but the results still indicate that SuperDARN velocities are on average lower than velocities measured by EISCAT. Comparisons with other instruments (such as the DMSP satellites) have also demonstrated lower SuperDARN velocities even after accounting for refractive index using the elevation angle proxy [*Gillies et al.*, 2009]. This would suggest that, although an estimate for the local scattering volume refractive index can significantly improve the SuperDARN velocity determination, a refinement of the technique or some further physical reasoning is needed to fully explain the systematic underestimate by SuperDARN of line-of-sight velocities.

[24] Another intriguing result from this study was the low correlation between n_s values obtained using the different methods. As discussed in the previous section, there is little correlation between n_s estimates from the different methods. An explanation for this lack of correlation is required as one may expect that they should deliver similar results.

4.2. Altitude Ambiguities

[25] A plausible explanation for the lack of correlation between n_s values could arise from the lack of precise knowledge about the altitude of SuperDARN scatter [*Chisham et al.*, 2008]. Slight variations in the scatter altitude would reduce the correlation between n_s values measured by EISCAT and those from the SuperDARN elevation angle. Since the elevation angle measurement is directly tied to the scattering location, estimates of n_s using elevation angle would differ from estimates using N_e measurements of the F-region peak if the scatter did not occur at the peak.

[26] The vertical gradient in N_e in the F region can be quite steep. To demonstrate the variation in scattering altitudes that is possible with SuperDARN, raytracing simulations through a model ionosphere have been performed. Figure 5 presents raypaths through a typical electron density profile that is presented beside the raypaths. The horizontal axis in Figure 5 represents an estimate of SuperDARN range gate and the vertical axis is altitude. Crosses on the raypaths represent points where the ray was within 1° of perpendicularity to the magnetic field lines, since coherent scattering requires high magnetic aspect sensitivity. At the ranges applicable for this study, the altitude at which scatter is possible can vary by up to ~100 km. Examination of the plot of N_e versus altitude (Figure 5, right) demonstrates that the electron density in the scattering region could range from $<2 \times 10^{11}$ m^{-3} (the density at ~200 km) to ~5×10^{11} m^{-3} (the density at ~280 km). At 12.5 MHz, this range of possible N_e values would result in n_s values of 0.95 and 0.85, respectively. This demonstrates that, under these conditions, using the peak density provided by IRI or EISCAT would result in a value of 0.85, although the actual value could be as high as 0.95. This would explain at least some of the lack of correlation between n_s predictions from the different methods. Note that although

the density profile used to produce Figure 5 is typical, the actual conditions can vary substantially and the locations of possible scatter would be different for different profiles. Figure 5 is simply meant to demonstrate the variability in scattering altitude that could occur under typical conditions.

4.3. Measurement Area Discrepancies

[27] Another plausible explanation for both the lack of agreement between the different methods to estimate n_s and the systematically lower SuperDARN velocities (even after attempts were made to account for n_s) involves the difference in measurement volumes between the two instruments. The electron density measurements from EISCAT occurred at a fixed location within the large SuperDARN range cell scattering volume. The beam width of EISCAT was 0.6°, which resulted in a scattering area of ~8 km^2 at an altitude of 280 km. The SuperDARN cell was 45 km in range and roughly 50 km wide at the range gates considered in this study. This results in a possible scattering area of more than 2000 km^2. Therefore the EISCAT measurement area was more than two orders of magnitude smaller than the SuperDARN measurement area.

[28] Not only did the size of the measurement areas differ, but the measurement techniques also differed. SuperDARN measured ionospheric velocities using coherent scattering from field-aligned irregularities. Therefore, SuperDARN scatter could occur in localized regions within the larger SuperDARN measurement volume. For example, it is possible that scatter occurred only in a small fraction of the SuperDARN cell in which conditions for scattering were appropriate. The main driver of field-aligned irregularities in the F region is the gradient drift instability that occurs in regions with electron density gradients. It is reasonable to assume that, compared to the well-behaved background electron density, localized structures with densities higher than background would produce stronger irregularities. In fact, a study of SuperDARN echoes in relation to polar cap patches has found that scatter tends to occur predominantly in regions with higher electron density [*Hosokawa et al.*, 2009]. These two behaviors indicate that coherent scatter from SuperDARN will be localized in regions with high electron densities and high gradients. Conversely, EISCAT measured the average electron density at a fixed location within the much larger SuperDARN cell. Therefore, on average, the EISCAT measurements of electron density would have delivered the average electron density in a SuperDARN cell, while SuperDARN measurements would have been biased to areas of the cell with high gradients and/or densities.

[29] The electron density in the auroral and polar regions of the F-region ionosphere can be quite structured. Small-scale structures with high gradients can form in the auroral region from processes such as particle precipitation and may be as small as hundreds of meters [e.g., *Noël et al.*, 2000, 2005; *Sofko et al.*, 2007]. In fact, any structure with scale sizes smaller than the 2000 km^2 size of a SuperDARN range cell would be important. On the dayside and over the polar cap, polar patches exist with regions of enhanced electron densities greater than 100% of the background level and scale sizes on the order of a few hundred kilometers. Although this scale is quite large, smaller structures are expected to develop within these patches [*Hosokawa et al.*, 2009]. Structure also exists in the region of the high-latitude ionospheric trough that, at least on the dayside, can be located poleward of the Hankasalmi SuperDARN radar location [e.g., *Sojka et al.*, 1990; *Pryse et al.*, 2005]. The poleward edge of the trough can produce an increase in electron density by an order of magnitude in a few tens of kilometers [e.g., *Mitchell et al.*, 1995]. Also of importance are traveling ionospheric disturbances (TIDs), which are wavelike structures in the ionosphere that also have scales of a few tens of kilometers and electron density enhancements of roughly 50%–100% [e.g., *Pryse et al.*, 1995].

[30] If SuperDARN scatter occurred in localized regions that had electron densities that were enhanced compared to the background values, then the actual value for N_e would be higher than the value predicted by the EISCAT measurement of N_e. Since a higher N_e value results in a lower n_s value, an enhanced N_e in the local scattering region will result in n_s values that are lower than those predicted using EISCAT. By equation (1) this would result in an underestimation of SuperDARN velocities compared to EISCAT velocities. If the electron density in the local SuperDARN scattering volume was systematically 50%–100% larger than the electron density predicted using EISCAT measurements, then the best fit slope line of Figure 4 would rise to unity and SuperDARN velocities would no longer be underestimated compared to EISCAT velocities. Although electron density perturbations of this magnitude on scale sizes comparable to a SuperDARN cell are possible (as discussed above), it may not be reasonable to expect that such structures existed for a large portion of the data points examined in this study. However, this effect at least partially explains the underestimation of SuperDARN velocities compared to EISCAT velocities even when attempts to account for n_s are made. Further, the fact that the two measurement volumes were of different sizes is one explanation for the lack of correlation between the different methods to estimate n_s because the EISCAT N_e measurement was essentially independent of the electron density in the effective SuperDARN scattering region. It should be noted that the preceeding argument dealt only with the N_e measurement by EISCAT and not the velocity measurement. It was assumed that even if electron density structures existed, the background velocity field was quite uniform throughout the range cell. This is the reason that the velocity comparisons had good correlation, but the n_s comparisons did not.

4.4. Horizontal Gradients

[31] The previous two suggestions for the lack of correlation between n_s estimates addressed problems that arose from using peak electron density measurements to determine n_s. It needs to be reiterated that using the elevation angle to determine n_s is only a proxy and therefore may not completely describe the situation. The estimate for n_s from the elevation angle as derived by *Gillies et al.* [2009] assumes that there were no horizontal gradients in electron density along the radar wave path. Clearly this assumption does not hold in all cases as the ionosphere is very dynamic and changes with latitude and longitude due to spatially dependent processes such as particle precipitation on the nightside and photoionization on the dayside. As a result, horizontal gradients may be important. *Gillies et al.* [2009]

used raypath simulations to demonstrate that, for even quite extreme large-scale (on the order of hundreds of kilometers) horizontal gradients, the elevation angle recorded by SuperDARN provides a reasonable estimate for n_s. Nevertheless, any deviation from the expected $\phi_o - n_s$ relationship due to horizontal gradients would also lower the correlation between n_s values estimated from elevation angle as compared to the other n_s estimations. *Gillies et al.* [2009] did not consider the effect of small-scale gradients, which, as discussed above, may be important.

4.5. Time Discrepancies Between Instruments

[32] The discrepancy between the integration times of the two instruments used in this study may also negatively impact the correlation. Recall that roughly 40% of the original comparison points were removed because there was high variability in the SuperDARN velocity values as compared to the surrounding SuperDARN cells. The comparison between EISCAT data integrated at 2-min intervals and SuperDARN single-beam data integrated for 3 or 7 s improved greatly when this removal was performed. The SuperDARN beams were sampled sequentially so that fast variations in velocities would have been apparent between neighboring beams. Such fast variations of velocity did occur for a large number of points, indicating that velocity changes on a timescale of just a few seconds were quite common in the SuperDARN scattering region.

[33] As the integration time of SuperDARN was under ~10 s and EISCAT had an integration time more than an order of magnitude longer at ~100 s, any velocity changes on a timescale shorter than the EISCAT integration time could result in a lack of correlation between SuperDARN and EISCAT measured velocity values. Therefore, at some times the instruments could conceivably measure different conditions in the ionosphere.

4.6. Ionospheric Heating Effects

[34] It is useful to note that in a study performed by *Eglitis et al.* [1998], use of the ionospheric heater at Tromsø resulted in good agreement between SuperDARN and EISCAT velocities with a slope value of 1.02 obtained. When the ionospheric heater was used, artificial irregularities were generated and detected by SuperDARN. These are expected to be more uniformly structured than natural auroral scattering regions. The SuperDARN radar would not have needed to rely on scatter from highly dense, presumably small-scale, spatially localized structures as the heater created irregularities throughout the scattering region from which the SuperDARN waves could scatter.

[35] Another effect of heating is the modification of the ambient electron density. At certain *F*-region altitudes it is expected that the electron density would decrease due to ionospheric heating increasing the recombination rate [e.g., *Rietveld et al.*, 1993]. A decrease in electron density would have brought the index of refraction closer to unity and caused less velocity underestimation by SuperDARN. Several studies have demonstrated an electron density depletion of 25%–50% created by lower latitude heating experiments at Arecibo [e.g., *Duncan et al.*, 1988; *Bernhardt et al.*, 1989; *Hansen et al.*, 1990; *Hansen et al.*, 1992]. A study by *Wright et al.* [1988] reported a density decrease of 15% due to heating at the higher latitude Tromsø facility. Conversely, *Stocker et al.* [1992] predicted and measured both increases and decreases of the electron density depending on several factors such as background electron density, heater frequency, and time of day. Further, the actual amount of electron density increase or decrease in the *Stocker et al.* [1992] study was quite low (less than 10%) which indicates that the refractive index was probably not affected greatly by this behavior. It would be beneficial to perform a more in-depth study of velocities measured by SuperDARN and EISCAT when the ionospheric heater is used.

5. Conclusions

[36] As a continuation of the work by *Gillies et al.* [2009], a comparison between SuperDARN line-of-sight velocities and EISCAT tristatic velocities has been performed. There was good correlation between the two data sets, but the velocities measured by SuperDARN tended to be lower than the corresponding velocities measured by EISCAT. This underestimation of velocities by SuperDARN was consistent with previous results [e.g., *Davies et al.*, 1999; *Drayton et al.*, 2005; *Drayton*, 2006]. This underestimate of line-of-sight velocities by SuperDARN was at least partially caused by the use of too high a value of the refractive index n_s in the scattering region. By using elevation angle measurements made by SuperDARN as a proxy for n_s, as proposed by *Gillies et al.* [2009], the best fit slope between SuperDARN and EISCAT velocities increased from 0.78 to 0.89 (an increase of 14%).

[37] One significant drawback to use of the elevation angle as a proxy for n_s is that these measurements are not always available. Therefore, other methods to estimate n_s were also considered. Electron density measurements by EISCAT and estimates from the IRI model were used to predict n_s, but these methods also have significant limitations. The EISCAT measurement of N_e was localized to a small area within one SuperDARN range cell and thus will typically not be of use to determine n_s in other parts of that range cell or for other range cells. The electron density value from IRI relied on large-scale mean estimates of N_e, thereby neglecting the higher densities expected in localized smaller-scale structures which cause coherent scatter.

[38] The two main issues raised from this comparison were the underestimation of velocities by SuperDARN even after elevation angle was used to estimate n_s and the lack of correlation between the different methods to estimate n_s. It is speculated that small-scale, highly dense structures in the SuperDARN scattering region partially explain both of these issues. These small-scale structures are important when they are of comparable size to the SuperDARN scattering volume. The small-scale structures cause strong irregularities from which the SuperDARN coherent radar waves scatter, while EISCAT incoherent radar measurements and IRI estimates of N_e provide only the background electron density and not the density of the small-scale structures, which are expected to be important in the coherent scattering process. Further, the altitude from which SuperDARN scattering occurs is known only approximately so it was difficult to select an appropriate value for N_e from either EISCAT or IRI. The angle-of-arrival proxy better accounts for both structures and the altitude ambiguity because the elevation angle measurements are directly linked

to the scattering region measurements. From this work, it can be inferred that SuperDARN scatter primarily occurs in localized regions with high electron density. It is also apparent that the modification of SuperDARN measured velocities due to the refractive index is larger than that based on the higher n_s values inferred from either the angle-of-arrival method or available electron density measurements.

[39] **Acknowledgments.** During this work RGG was supported by the Canadian Space Agency and the Natural Sciences and Engineering Research Council (NSERC) to the Canadian component of the SuperDARN ground based radar system and the CASSIOPE/ePOP project and by the EU Marie Curie Early Stage Training in Space, Planetary and Astrophysical Sciences (SPARTAN) Programme. The CUTLASS (Co-operative UK Twin Located Auroral Sounding System) radars form part of the SuperDARN (Dual Auroral Radar Network) HF project and consist of radars at Hankasalmi (Finland) and Pykkvibaer (Iceland). They are operated by the Radio and Space Plasma Physics Group at the University of Leicester with support from the Particle Physics and Astronomy Council and additional support from the Finnish Meteorological Institute and the Swedish Meteorological Institute. We are indebted to the Director and staff of EISCAT for operating the facility and supplying the data. EISCAT is an International Association supported by Finland (SA), France (CNRS), Germany (MPG), Japan (NIPR), Norway (NFR), Sweden (VR), and the United Kingdom (PPARC). During this work DMW was supported by the UK Science and Technology Facilities Council (Grant Number: PP/E000983).

[40] Zuyin Pu thanks William Bristow and another reviewer for their assistance in evaluating this paper.

References

André, D., G. Sofko, K. Baker, and J. MacDougall (1998), SuperDARN interferometry: Meteor echoes and electron densities from groundscatter, *J. Geophys. Res.*, *103*, 7003–7015.

Baker, K. B., J. R. Dudeney, R. A. Greenwald, M. Pinnick, P. T. Newell, A. S. Rodger, N. Mattin, and C.-I. Meng (1995), HF radar signatures of the cusp and low-latitude boundary layer, *J. Geophys. Res.*, *100*, 7671–7695.

Bernhardt, P. A., C. A. Teply, and L. M. Duncan (1989), Airglow enhancements associated with plasma cavities formed during ionospheric heating experiments, *J. Geophys. Res.*, *94*, 9071–9092.

Bilitza, D. (2001), International Reference Ionosphere 2000, *Radio Sci.*, Vol. 36, 261–275.

Budden, K. G. (1961), *Radio Waves in the Ionosphere*, Cambridge University Press, Cambridge, U. K.

Chisham, G., T. K. Yeoman, and G. J. Sofko (2008), Mapping ionospheric backscatter measured by the SuperDARN HF radars. Part 1: A new empirical virtual height model, *Ann. Geophys.*, *26*, 823–841.

Davies, J. A., M. Lester, S. E. Milan, and T. K. Yeoman (1999), A comparison of velocity measurements from the CUTLASS Finland radar and the EISCAT UHF system, *Ann. Geophys.*, *17*, 892–902.

Drayton, R. A. (2006), Study of SAPS-like flows with the King Salmon SuperDARN radar, M.Sc. thesis, Institute of Space and Atmospheric Studies, Univ. of Saskatchewan, Saskatchewan.

Drayton, R. A., A. V. Koustov, M. R. Hairston, and J.-P. Villian (2005), Comparison of DMSP cross-track ion drifts and SuperDARN line-of-sight velocities, *Ann. Geophys.*, *23*, 2479–2489.

Duncan, L. M., J. P. Sheerin, and R. A. Behnke (1988), Observations of ionospheric cavities generated by high-power radio waves, *Phys. Rev. Lett.*, *61*, 239–242, 1988.

Eglitis, P., T. R. Robinson, M. T. Rietveld, D. M. Wright, and G. E. Bond (1998), The phase speed of artificial field-aligned irregularities observed by CUTLASS during HF modification of the auroral ionosphere, *J. Geophys. Res.*, *103*, 2253–2259.

Gillies, R. G., G. C. Hussey, G. J. Sofko, K. A. McWilliams, R. A. D. Fiori, P. Ponomarenko, and J.-P. St. Maurice (2009), Improvement of SuperDARN velocity measurements by estimating the index of refraction in the scattering region using interferometry, *J. Geophys. Res.*, *114*, A07305, doi:10.1029/2008JA013967.

Ginzburg, V. L. (1964), *The Propagation of Electromagnetic Waves in Plasmas*, Pergamon Press, New York.

Greenwald, R. A., et al. (1995), DARN/SuperDARN: A global view of the dynamics of high-latitude convection, *Space Sci. Rev.*, *71*, 761–796.

Haldoupis, C., and K. Schlegel (1990), Direct comparison of 1-m irregularity phase velocities and ion acoustic speeds in the auroral *E*-region ionosphere, *J. Geophys. Res.*, *95*, 989–1000.

Hansen, J. D., G. J. Morales, L. M. Duncan, J. E. Maggs, and G. Dimonte (1990), Large-scale ionospheric modifications produced by nonlinear refractions of an hf wave, *Phys. Rev. Lett.*, *65*, 3285–3288.

Hansen, J. D., G. J. Morales, L. M. Duncan, and G. Dimonte (1992), Large-scale HF-induced ionospheric modifications: experiments, *J. Geophys. Res.*, *97*, 113–122.

Hosokawa, K., K. Shiokawa, Y. Otsuka, T. Ogawa, J.-P. St-Maurice, G. J. Sofko, and D. A. Andre (2009), Relationship between polar cap patches and field-aligned irregularities as observed with an all-sky airglow imager at Resolute Bay and the PolarDARN radar at Rankin Inlet, *J. Geophys. Res.*, *114*, A03306, doi:10.1029/2008JA013707.

Mitchell, C. N., D. G. Jones, L. Kersley, S. E. Pryse, and I. K. Walker (1995), Imaging of field-aligned structures in the auroral ionopshere, *Ann. Geophys.*, *13*, 1311–1319.

Milan, S. E., T. B. Jones, T. R. Robinson, E. C. Thomas, and T. K. Yeoman (1997), Interferometric evidence for the observation of ground backscatter originating behind the CUTLASS coherent radars, *Ann. Geophys.*, *15*, 29–39.

Noël, J.-M. A., J.-P. St. Maurice, and P.-L. Blelly (2000), Nonlinear model of short-scale electrodynamics in the auroral ionosphere, *Ann. Geophys.*, *18*, 1128–1144.

Noël, J.-M. A., J.-P. St. Maurice, and P.-L. Blelly (2005), The effect of *E*-region wave heating on electrodynamical structures, *Ann. Geophys.*, *23*, 2081–2094.

Pryse, S. E., C. N. Mitchell, J. A. Heaton, and L. Kersley (1995), Travelling ionospheric disturbances imaged by tomographic techniques, *Ann. Geophys.*, *13*, 1325–1330.

Pryse, S. E., K. L. Dewis, R. L. Balthazor, H. R. Middleton, and M. H. Denton (2005), The dayside high-latitude trough under quiet geomagnetic conditions: Radio tomography and the CTIP model, *Ann. Geophys.*, *23*, 1199–1206, 2005.

Rietveld, M. T., H. Kohl, H. Kopka, and P. Stubbe (1993), Introduction to ionospheric heating at Tromsø. I. Experimental overview, *J. Atmos. Terr. Phys.*, *55*, 577–599.

Rishbeth, H., and A. P. van Eyken (1993), EISCAT: Early history and the first ten years of operation, *J. Atmos. Terr. Phys.*, *55*, 525–542.

Robinson, T. R. (1989), The heating of the high latitude ionosphere by high power radio waves, *Phys. Rep.*, *179*, 79–209.

Sofko, G., R. Schwab, M. Watanabe, C. Huang, J. Foster, and K. McWilliams (2007), Auroral post-secondary ions from the nightside ionosphere in the inner magnetosphere, *J. Atmos. Sol. Terr. Phys.*, *69*, 1213–1232.

Sojka, J. J., R. W. Schunk, and J. A. Whalen (1990), The longitude dependence of the dayside *F* region trough: A detailed model-observation comparison, *J. Geophys. Res.*, *95*, 15,275–15,280.

Stocker, A. J., F. Honary, T. R. Robinson, T. B. Jones, P. Stubbe, and H. Kopka (1992), EISCAT observations of large scale electron temperature and electron density perturbations caused by high power HF radio waves, *J. Atmos. Terr. Phys.*, *54*, 1555–1572.

Stubbe, P. (1996), Review of ionospheric modification experiments at Tromsø, *J. Atmos. Terr. Phys.*, *58*, 349–368.

Wright, J. W., H. Kopka, and P. Stubbe (1988), A large-scale ionospheric depletion by intense radio wave heating, *Geophys. Res. Lett.*, *15*, 1531–1533.

Xu, L., A. V. Koustov, J. Thayer, and M. A. McCready (2001), SuperDARN convection and Sondrestrom plasma drift, *Ann. Geophys.*, *19*, 749–759.

J. A. Davies, Space Science and Technology Department, Rutherford Appleton Laboratory, Harwell Science and Innovation Campus, Didcot OX11 0QX, UK.

R. G. Gillies, G. C. Hussey, and G. J. Sofko, Institute of Space and Atmospheric Science, University of Saskatchewan, 116 Science Pl., Saskatoon, SK S7N 5E2, Canada. (Rob.Gillies@usask.ca)

D. M. Wright, Department of Physics and Astronomy, University of Leicester, University Road, Leicester LE1 7RH, UK.